# Erratum: Collapse of Coherent Large Scale Flow in Strongly Turbulent Liquid Metal Convection [Phys. Rev. Lett. 128, 164501 (2022)]

Felix Schindler, Sven Eckert, Till Zürner, Jörg Schumacher, and Tobias Vogt

(Received 10 July 2023; published 9 October 2023)

DOI: 10.1103/PhysRevLett.131.159901

This Erratum reports an error found in the experimental setup that affected the results published in this Letter. The error concerned the accuracy of the temperature measurements at the top and bottom plates of the aspect ratio $\Gamma = 0.5$ convection cell and therefore affected the Rayleigh and Nusselt number measurements presented in our Letter. We corrected the error and present the reproduced measurements in this Erratum. The main conclusion, that there is no stable large scale circulation (LSC) in strongly turbulent liquid metal convection in the aspect ratio $\Gamma = 0.5$, remains.

In the original $\Gamma = 0.5$ setup, the liquid metal was separated from the temperature-controlled copper plates by a thin layer of acrylic varnish to prevent intermetallic reactions. The varnish layer was supposed to be only a few micrometers thick, so that it does not present any relevant thermal resistance. During a revision of the experiment, the thickness of the varnish film was determined and found to be $60 \pm 6$ μm, which is significantly thicker than originally assumed. This relatively thick varnish layer affects the effective $\Delta T$ across the liquid metal layer, since large temperature gradients occur in the varnish layer. The measured temperature gradient in the liquid metal is thus erroneous in the original publication, affecting the Rayleigh number (Ra) and more strongly the Nusselt number (Nu).

To eliminate the influence of the varnish layer on the results, the layer was removed and new measurement series were recorded where the liquid metal was in direct contact with the copper plates. Even without the varnish layer, no stable LSC develops in $\Gamma = 0.5$ [Fig. 2(c)]. The influence of the varnish layer on the dynamics of the LSC seems to be negligible and the main statement of our Letter, that the LSC in strongly turbulent liquid metal convection flows collapses in $\Gamma = 0.5$, is still valid. However, relevant changes occur in the Re scaling [Fig. 5(a)] and even more in the Nu scaling [Fig. 5(b)]. The updated Nusselt-Rayleigh scaling $\mathrm{Nu} \propto \mathrm{Ra}^{0.275}$ is now in good agreement with $\mathrm{Nu} \propto \mathrm{Ra}^{0.285}$ measured in mercury in $\Gamma = 0.5$ [1]. An updated data table for the reproduced measurements with uncoated copper plates at the top and bottom of the convection cell can be found in Table I.

This work is supported by the Deutsche Forschungsgemeinschaft with Grants No. VO 2332/1-1 and No. SCHU 1410/29-1.

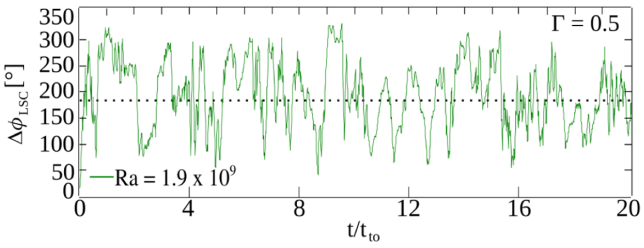


FIG. 2. (c) Large-scale flow analysis. Angular difference $\Delta\phi_{\mathrm{LSC}} \in [0°, 360°]$ of the flow direction at the top and bottom plate vs time normalized by the turnover time $t_{\mathrm{to}}$ for $\mathrm{Ra} = 1.9 \times 10^9$ in the $\Gamma = 0.5$ cell with uncoated copper plates, revealing frequent nonperiodic changes between various flow states.

 

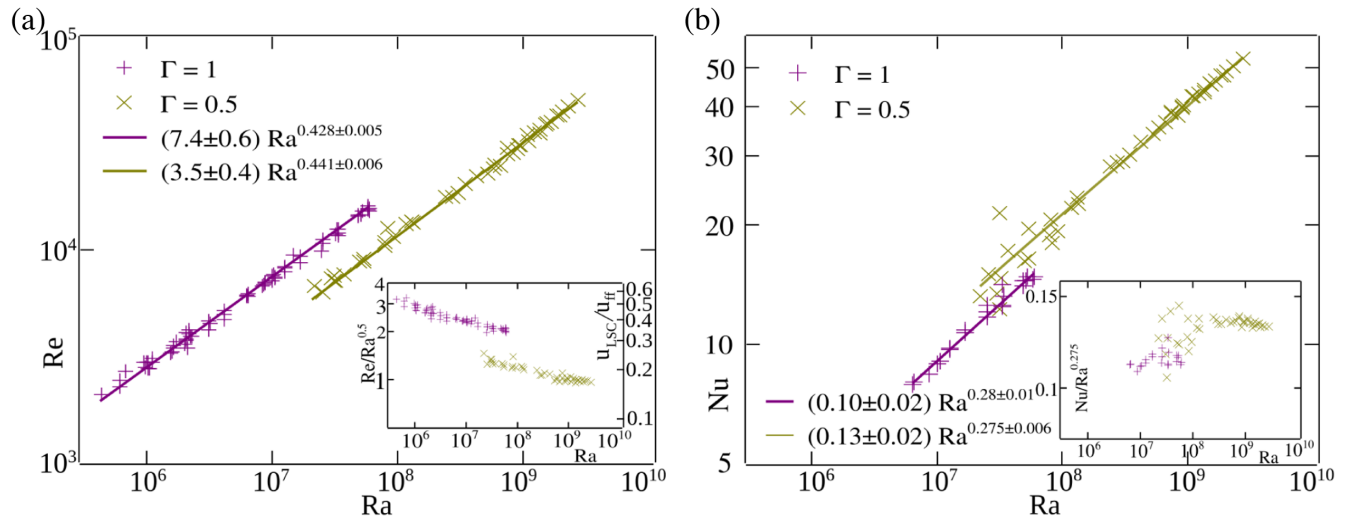


FIG. 5. Global transport laws. (a) Reynolds number Re versus Rayleigh number Ra. Inset: compensated plot of $\mathrm{Re}/\mathrm{Ra}^{1/2}$ and corresponding $u_{\mathrm{LSC}}/u_{ff}$ versus Ra. (b) Nusselt number Nu versus Ra. Inset: compensated plot $\mathrm{Nu}/\mathrm{Ra}^{0.275}$ versus Ra.

TABLE I. Data table for the new conducted laboratory experiments at aspect ratio $\Gamma = 0.5$ with uncoated copper plates at the top and bottom. First and second columns show the Rayleigh number Ra and the corresponding standard deviation $\sigma(\mathrm{Ra})$, the next column shows the Prandtl number Pr, the fourth and fifth columns show the Reynolds numbers Re and the corresponding standard deviation $\sigma(\mathrm{Re})$. The sixth and seventh columns show the Nusselt number Nu and the corresponding standard deviation $\sigma(\mathrm{Nu})$. Columns eight through eleven show the temperatures and standard deviations for the bottom and top temperatures in units of degrees Celsius. The last column shows the temperature difference between the bottom and the top in Kelvin.

| Ra | $\sigma(\mathrm{Ra})$ | Pr | Re | $\sigma(\mathrm{Re})$ | Nu | $\sigma(\mathrm{Nu})$ | $T_{\mathrm{Bot}}$ | $\sigma(T_{\mathrm{Bot}})$ | $T_{\mathrm{Top}}$ | $\sigma(T_{\mathrm{Top}})$ | $\Delta T$ |
|---|---|---|---|---|---|---|---|---|---|---|---|
| $2.19e+07$ | $7.43e+05$ | 0.032 | $6.81e+03$ | $2.57e+03$ | 13.23 | 2.74 | 23.69 | 0.01 | 23.45 | 0.01 | 0.24 |
| $2.57e+07$ | $9.7e+05$ | 0.0327 | $6.35e+03$ | $2.23e+03$ | 15.09 | 2.68 | 21.08 | 0.01 | 20.80 | 0.01 | 0.28 |
| $3.01e+07$ | $9.45e+05$ | 0.0329 | $7.36e+03$ | $2.54e+03$ | 13.46 | 2.98 | 20.28 | 0.01 | 19.94 | 0.01 | 0.33 |
| $3.13e+07$ | $2.03e+06$ | 0.0327 | $7.17e+03$ | $2.84e+03$ | 21.41 | 6.38 | 21.23 | 0.02 | 20.89 | 0.02 | 0.34 |
| $3.14e+07$ | $7.61e+05$ | 0.0317 | $7.52e+03$ | $2.62e+03$ | 12.27 | 3.32 | 24.79 | 0.01 | 24.45 | 0.01 | 0.34 |
| $3.25e+07$ | $1.08e+06$ | 0.0327 | $7.17e+03$ | $2.57e+03$ | 14.73 | 2.94 | 21.07 | 0.01 | 20.71 | 0.01 | 0.36 |
| $3.72e+07$ | $1.18e+06$ | 0.0332 | $7.65e+03$ | $2.66e+03$ | 17.25 | 3.20 | 19.44 | 0.01 | 19.03 | 0.01 | 0.41 |
| $4.96e+07$ | $1.53e+06$ | 0.0317 | $8.86e+03$ | $2.91e+03$ | 16.20 | 2.89 | 25.01 | 0.01 | 24.47 | 0.01 | 0.54 |
| $5.38e+07$ | $1.54e+06$ | 0.0332 | $8.8e+03$ | $2.9e+03$ | 19.59 | 2.80 | 19.45 | 0.01 | 18.86 | 0.01 | 0.59 |
| $5.42e+07$ | $1.87e+06$ | 0.0327 | $9.1e+03$ | $3.04e+03$ | 16.54 | 3.71 | 21.03 | 0.01 | 20.43 | 0.02 | 0.59 |
| $7.88e+07$ | $2.44e+06$ | 0.0315 | $1.05e+04$ | $3.36e+03$ | 18.96 | 2.93 | 25.97 | 0.02 | 25.11 | 0.02 | 0.86 |
| $8.02e+07$ | $2.63e+06$ | 0.0331 | $1.08e+04$ | $3.51e+03$ | 20.66 | 3.14 | 19.79 | 0.02 | 18.90 | 0.02 | 0.88 |
| $8.3e+07$ | $2.75e+06$ | 0.0321 | $1.27e+04$ | $4.24e+03$ | 18.06 | 3.61 | 23.75 | 0.02 | 22.85 | 0.02 | 0.91 |
| $9.31e+07$ | $2.89e+06$ | 0.0315 | $1.15e+04$ | $3.57e+03$ | 19.40 | 3.04 | 26.03 | 0.02 | 25.02 | 0.02 | 1.01 |
| $1.18e+08$ | $4.38e+06$ | 0.0318 | $1.32e+04$ | $4.57e+03$ | 22.08 | 3.87 | 24.96 | 0.03 | 23.67 | 0.03 | 1.29 |
| $1.3e+08$ | $4.3e+06$ | 0.0321 | $1.36e+04$ | $4.54e+03$ | 23.59 | 2.84 | 24.07 | 0.03 | 22.65 | 0.02 | 1.42 |
| $1.33e+08$ | $4.14e+06$ | 0.0331 | $1.33e+04$ | $4.11e+03$ | 22.67 | 2.96 | 20.30 | 0.03 | 18.83 | 0.03 | 1.47 |
| $2.41e+08$ | $8.08e+06$ | 0.0328 | $1.78e+04$ | $5.23e+03$ | 28.12 | 2.81 | 21.85 | 0.05 | 19.20 | 0.05 | 2.65 |
| $2.77e+08$ | $9.36e+06$ | 0.033 | $1.78e+04$ | $5.64e+03$ | 28.89 | 2.95 | 21.27 | 0.06 | 18.22 | 0.05 | 3.05 |
| $3.02e+08$ | $1.11e+07$ | 0.033 | $1.84e+04$ | $5.91e+03$ | 29.07 | 3.15 | 21.50 | 0.07 | 18.18 | 0.06 | 3.33 |
| $3.43e+08$ | $1.13e+07$ | 0.0323 | $2.03e+04$ | $5.92e+03$ | 30.11 | 2.92 | 24.26 | 0.08 | 20.52 | 0.07 | 3.75 |
| $4.2e+08$ | $1.62e+07$ | 0.0325 | $2.21e+04$ | $7.38e+03$ | 32.46 | 3.31 | 24.05 | 0.10 | 19.46 | 0.09 | 4.60 |
| $5.29e+08$ | $1.91e+07$ | 0.0324 | $2.27e+04$ | $7.46e+03$ | 34.06 | 3.04 | 24.78 | 0.12 | 18.99 | 0.10 | 5.79 |
| $5.84e+08$ | $2.21e+07$ | 0.0323 | $2.42e+04$ | $7.54e+03$ | 35.25 | 3.48 | 25.56 | 0.14 | 19.17 | 0.12 | 6.39 |
| $5.89e+08$ | $2.06e+07$ | 0.0324 | $2.5e+04$ | $7.86e+03$ | 35.33 | 2.96 | 25.18 | 0.13 | 18.74 | 0.12 | 6.44 |
| $6.61e+08$ | $2.37e+07$ | 0.0314 | $2.49e+04$ | $8.41e+03$ | 36.58 | 3.13 | 29.61 | 0.15 | 22.44 | 0.14 | 7.17 |
| $7.46e+08$ | $2.64e+07$ | 0.032 | $3e+04$ | $9.06e+03$ | 38.33 | 3.03 | 27.54 | 0.17 | 19.40 | 0.14 | 8.14 |
| $7.5e+08$ | $3.95e+07$ | 0.0312 | $2.8e+04$ | $9.15e+03$ | 38.69 | 3.56 | 30.94 | 0.38 | 22.82 | 0.15 | 8.12 |
| $8.39e+08$ | $3.21e+07$ | 0.031 | $2.83e+04$ | $9.66e+03$ | 37.99 | 3.25 | 32.10 | 0.21 | 23.03 | 0.18 | 9.07 |
| $9.08e+08$ | $3.43e+07$ | 0.0317 | $2.96e+04$ | $1e+04$ | 39.62 | 3.23 | 29.80 | 0.22 | 19.92 | 0.18 | 9.87 |
| $9.11e+08$ | $3.47e+07$ | 0.0316 | $3.09e+04$ | $1.03e+04$ | 39.88 | 3.23 | 29.88 | 0.23 | 19.97 | 0.19 | 9.91 |
| $9.41e+08$ | $3.36e+07$ | 0.0304 | $3.12e+04$ | $1.02e+04$ | 40.33 | 3.42 | 35.00 | 0.22 | 24.88 | 0.18 | 10.11 |
| $1.09e+09$ | $4.04e+07$ | 0.0305 | $3.44e+04$ | $1.17e+04$ | 42.36 | 3.29 | 35.33 | 0.25 | 23.60 | 0.22 | 11.73 |
| $1.11e+09$ | $4.23e+07$ | 0.0301 | $3.24e+04$ | $1.07e+04$ | 42.32 | 3.51 | 37.32 | 0.27 | 25.43 | 0.22 | 11.89 |
| $1.24e+09$ | $4.38e+07$ | 0.0298 | $3.57e+04$ | $1.14e+04$ | 43.15 | 3.58 | 39.07 | 0.28 | 25.83 | 0.23 | 13.24 |
| $1.35e+09$ | $5.18e+07$ | 0.0296 | $3.51e+04$ | $1.18e+04$ | 43.93 | 3.43 | 40.66 | 0.36 | 26.22 | 0.26 | 14.43 |
| $1.36e+09$ | $4.8e+07$ | 0.0291 | $3.68e+04$ | $1.29e+04$ | 43.30 | 3.69 | 42.66 | 0.31 | 28.23 | 0.25 | 14.43 |
| $1.52e+09$ | $5.78e+07$ | 0.0293 | $3.86e+04$ | $1.32e+04$ | 45.83 | 3.75 | 43.02 | 0.36 | 26.83 | 0.30 | 16.18 |
| $1.56e+09$ | $6.05e+07$ | 0.0287 | $3.9e+04$ | $1.38e+04$ | 45.44 | 3.99 | 45.52 | 0.37 | 29.00 | 0.32 | 16.52 |
| $1.66e+09$ | $6.6e+07$ | 0.0291 | $3.96e+04$ | $1.29e+04$ | 46.52 | 3.62 | 44.66 | 0.47 | 27.03 | 0.35 | 17.62 |
| $1.83e+09$ | $6.84e+07$ | 0.028 | $4.29e+04$ | $1.47e+04$ | 47.88 | 3.71 | 50.29 | 0.42 | 30.99 | 0.35 | 19.29 |
| $1.94e+09$ | $7.09e+07$ | 0.0284 | $4.25e+04$ | $1.49e+04$ | 47.92 | 3.52 | 49.23 | 0.45 | 28.75 | 0.37 | 20.48 |
| $2.06e+09$ | $7.46e+07$ | 0.0276 | $4.47e+04$ | $1.49e+04$ | 49.02 | 3.47 | 53.41 | 0.47 | 31.82 | 0.37 | 21.59 |
| $2.3e+09$ | $8.8e+07$ | 0.0272 | $4.74e+04$ | $1.6e+04$ | 50.41 | 3.73 | 56.80 | 0.53 | 32.73 | 0.45 | 24.07 |
| $2.75e+09$ | $1.01e+08$ | 0.0266 | $5.06e+04$ | $1.74e+04$ | 52.82 | 3.68 | 62.01 | 0.60 | 33.40 | 0.54 | 28.61 |

[1] J. Glazier, T. Segawa, A. Naert, and M. Sano, Evidence against 'ultrahard' thermal turbulence at very high Rayleigh numbers, Nature (London) **398**, 307 (1999).